1.SUPPLEMENTARY FIGURES AND LEGENDS

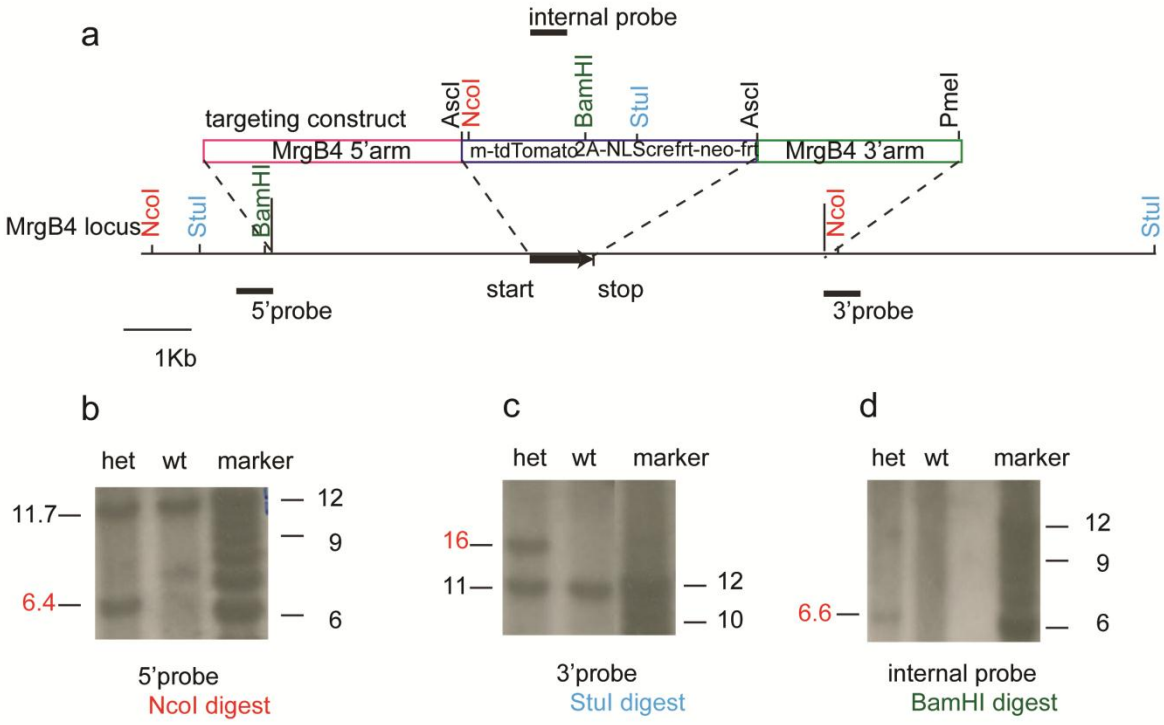

Supplementary Figure S1. Generation of MrgprB4 knockout mice. a, A targeting construct containing the m-tdTomato-2A-NLSCre-frt-neo-frt cassette, illustrated in the upper diagram, was designed to replace the entire open reading frame (ORF) of MrgprB4 (large arrow in the lower diagram, representing the MrgprB4 locus) following homologous recombination (dashed lines). **b,** Genomic DNA from wild type (wt) and MrgprB4$^{tdTomato\text{-}2A\text{-}Cre/+}$ heterozygous mice was digested, Southern blotted and hybridized with probes shown in (**a**) to confirm the homologous recombination event. Sizes are in kb. Bands predicted by correct homologous recombination event are in red.

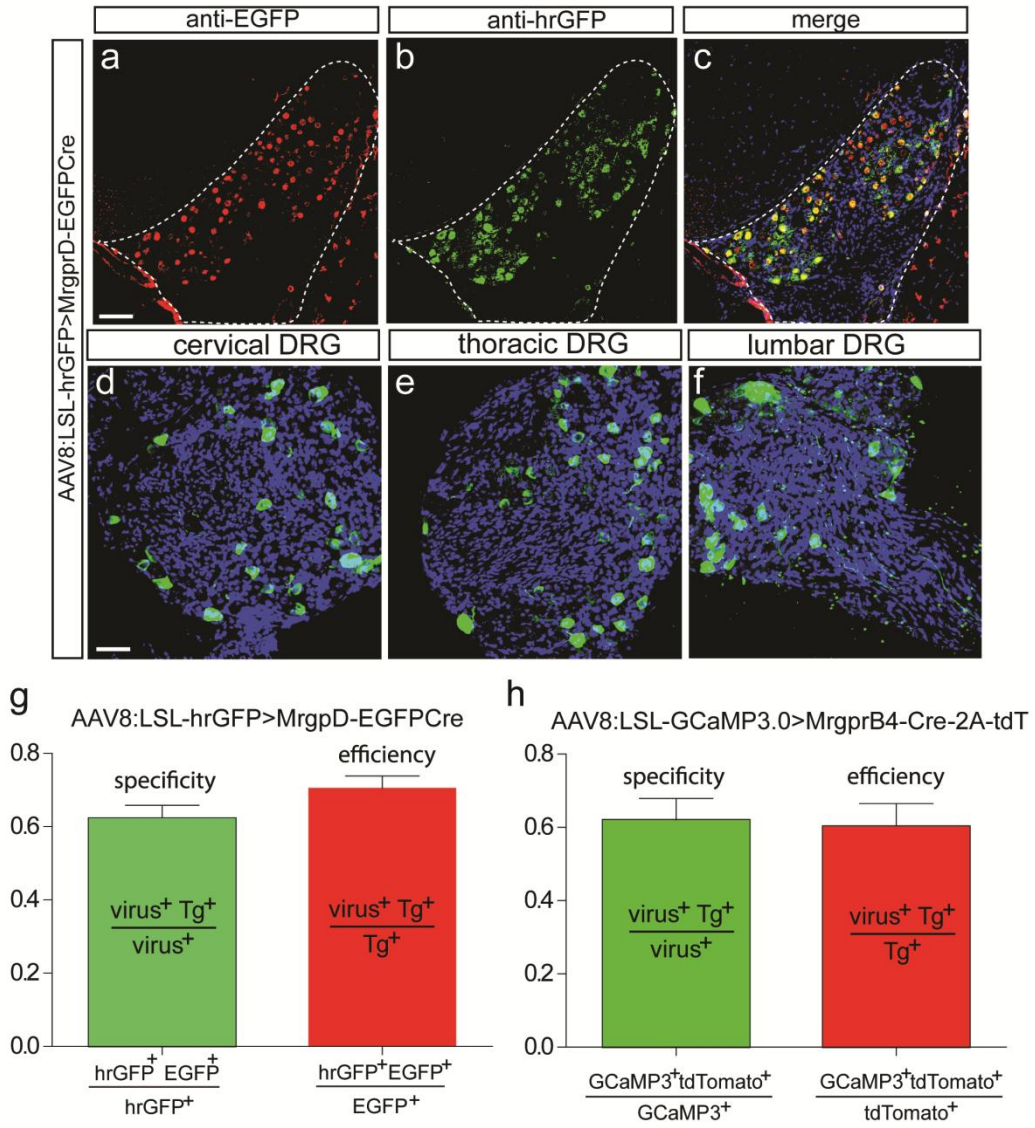

Supplementary Figure S2. Specificity and efficiency of the neonatal virus injections. (**a-c**) Visualization of EGFP transgene expression (anti-EGFP) and viral hrGFP expression in the DRG of adult *MrgprD-EGFPCre* mice injected neonatally with a Cre-dependent AAV8 virus expressing hrGFP. The signal outside of the DRG in (**a**) (dashed outline) is autofluorescence, pseudocolored red. (**d-f**) Similarly prepared mice showing expression of viral hrGFP expression in ganglia across the rostro-caudal axis. Scale bars in (**a-c**) and (**d-f**) are 55 and 35 µm, respectively. No expression of hrGFP was detected in wild-type mice injected with the Cre-

dependent AAV8:hrGFP (not shown). Bar graphs in (**g, h**) indicate the specificity and efficiency of Cre-dependent virus expression in adult MrgprD-EGFPCre (**g**) and MrgprB4-tdTomato-2A-Cre (**h**) mice, following neonatal i.p. injections with Cre-dependent hrGFP and Cre-dependent GCaMP3 virus respectively. LSL denotes loxP-STOP-loxP cassette. In the case of MrgprD-EGFPCre mice, Cre-dependent AAV8:hrGFP was used rather than GCaMP3.0 to enable independent antibody staining of the transgene (EGFP) and viral reporter (hrGFP).

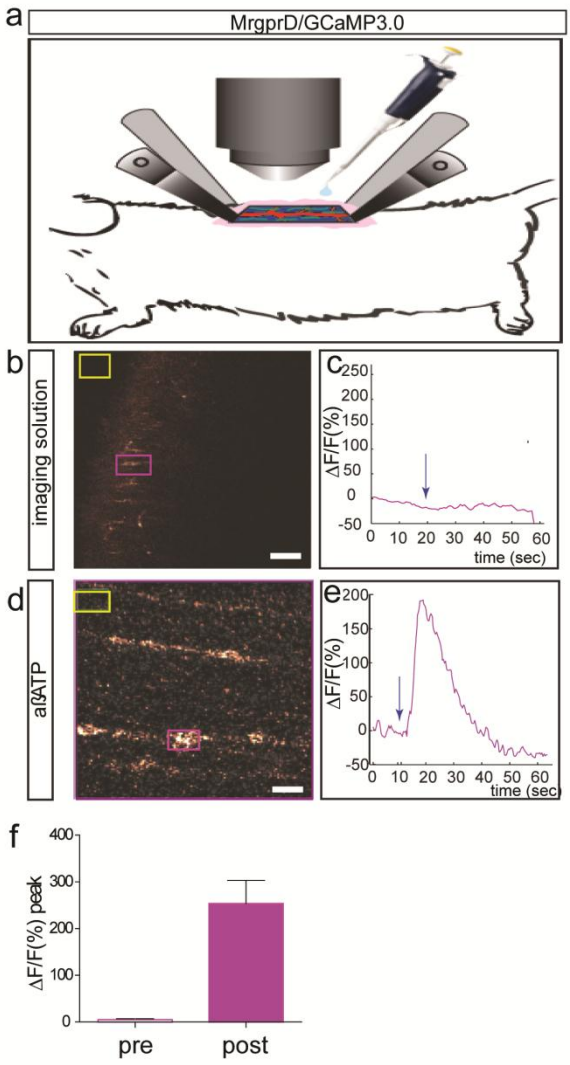

Supplementary Figure S3. Activation of MrgprD$^+$ fibers by α, β-methyl ATP application to the spinal cord. a, Schematic illustrating application of chemical solutions to the spinal cord (not to scale). (**b, c**) Application of imaging solution (**c,** blue arrow) did not evoke calcium transient in the same ROI as used for imaging of KCl responses (**b**; cf. Fig. **1i, j**). (**d, e**) Application of α, β-methyl ATP to the spinal cord of MrgD mice induced a strong calcium response (**e**). ROI used for imaging is magenta rectangle, yellow rectangle is region used for background subtraction (**b, d**). (**f**) Bar graph of peak ΔF/F values before (open bar) vs. after (filled bar) stimulation. n=2, mean±range. Scale bars, in (**b, d**) are 40 and 5.5 µm respectively.

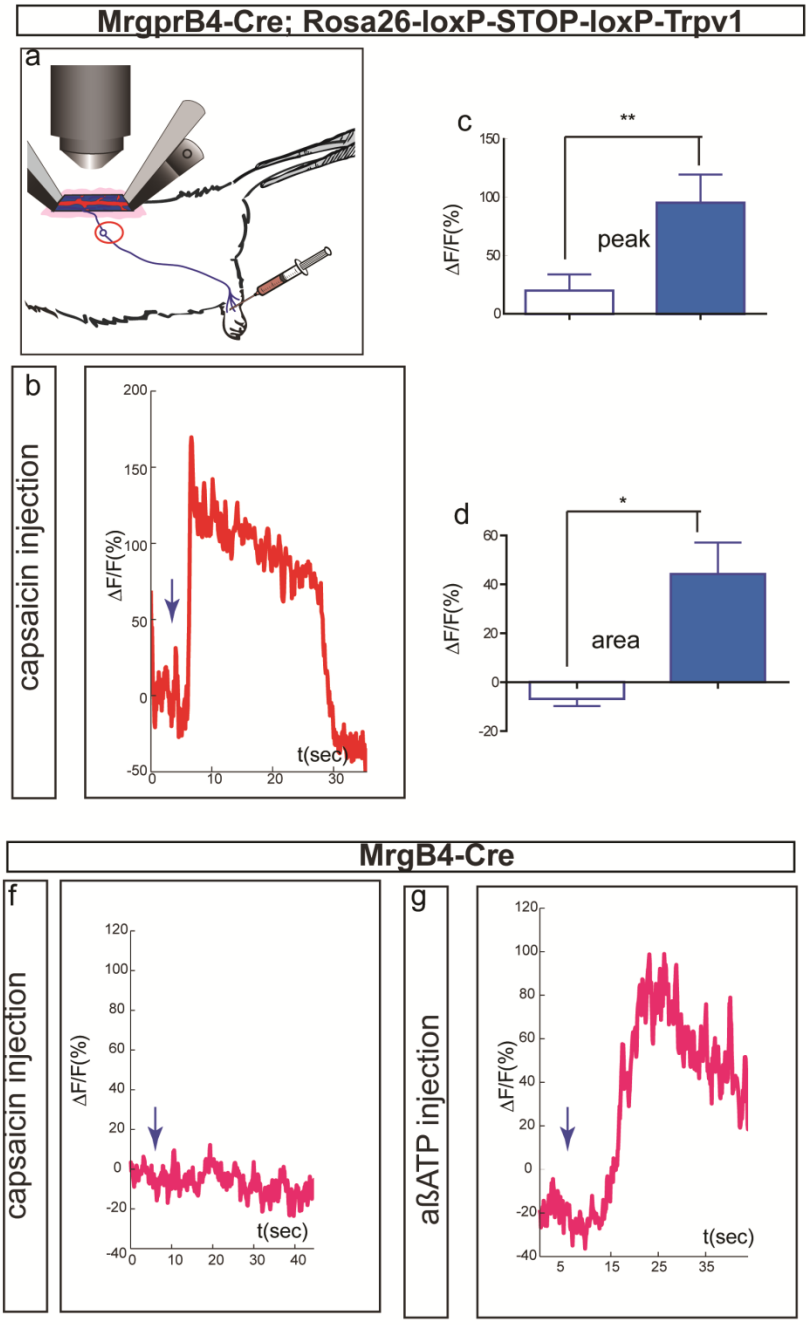

Supplementary Figure S4. Imaging activity after peripheral injection of capsaicin in *MrgprB4-Cre x Rosa-loxPSTOPloxP-TRPV1* mice.

(a), Schematic illustrating peripheral injection of capsaicin or α, β-methylene ATP into hairy skin of hindlimb. **(b)**, Calcium transients in the central afferent fibers of mice expressing GCaMP3.0 and TRPV1 receptor in MrgprB4^{+} neurons, evoked by peripheral injection of

capsaicin. (**c, d**) Quantification of peak ΔF/F values or integrated area, before (open bars) vs. after (filled bars) capsaicin injections from 4 different animals (paired t-tests)). Data shown are mean±SEM). (**f, g**) Mice expressing GCaMP3.0 but not the TRPV1 receptor in MrgprB4^{+} neurons, exhibit calcium transients evoked by peripheral injection of α, β-methylene ATP (**g**), but not with capsaicin in the same field of view (**f**) (the injections were performed with a 15-20 min window so as to avoid desensitization from capsaicin). Blue arrows (**b, f, g**) indicate time of stimulus delivery.

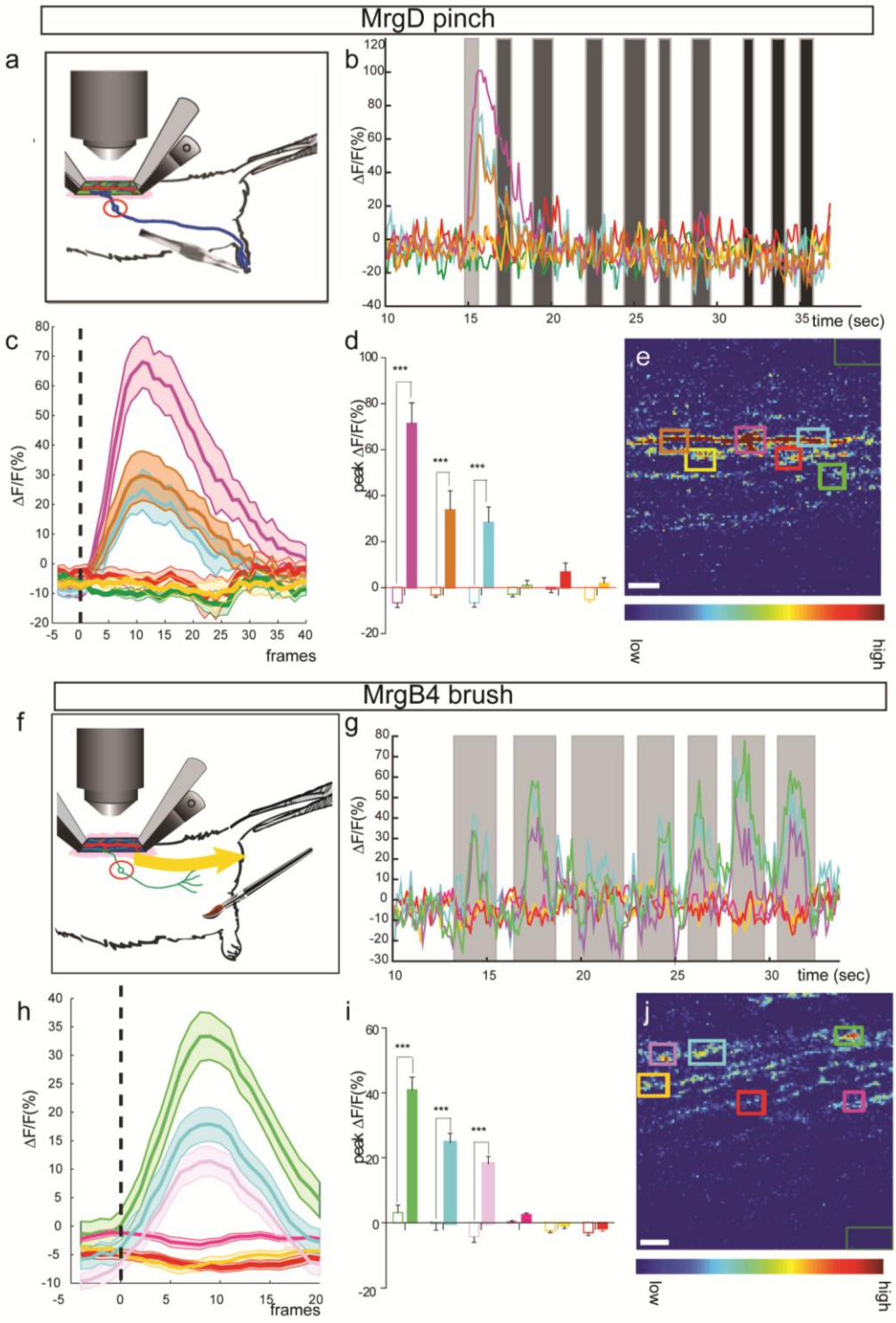

Supplementary Figure S5. MrgprD^{+} and MrgprB4^{+} fibers are activated by mechanical stimuli in multiple ROIs in a given field of view. a, f, Schematics illustrating pinching (**a**) and

stroking (**f**) stimuli. **e, j** ROIs used for imaging in (**b-d)** and (**g-i)**, respectively. Dark green rectangles (upper right in **e**, and lower right in **j**,) are regions used for background subtraction. **b**, Superimposed traces from different color-coded ROIs (**e**) in a single trial consisting of 10 pinch stimuli. Light gray bar represents pinching in a specific ipsilateral digit where the stimulus evoked a response, dark gray bars represent pinching in other ipsilateral digits (see also Supplementary Fig. 6g-l), black bars represent pinching in contralateral digits (see also Supplementary Fig. 6a-f). **c**, Trial average for response to pinching (n=4 trials, 1-4 stimuli/trial), from a single animal. **d,** MPI $\Delta F/F_{peak}$ calculated from the curves in (**c**). **g**, Superimposed traces from different color-coded ROIs (**j**) in a single trial consisting of 7 brushing stimuli (light gray bars). The onset of the rise in $\Delta F/F$ is variably offset from the apparent onset of the stimulus (left edge of gray bars), because the stimulus time stamp pulse is manually actuated (by squeezing the brush between the thumb and forefinger at a specific contact point), and there is some variation in the time elapsed between this actuation and the actual stimulus application to the animal. Alternatively, the receptive field of the activated fiber might lie towards the middle or end of the path of the brush stimulus, and therefore activation would be observed later in the stimulus delivery period. **h**, Trial average for response to brushing (n=5 trials, ~6 stimuli/trial), from a single animal. **i,** MPI $\Delta F/F_{peak}$ calculated from the curves in (**h**). Open and filled bars in (**d)** and (**i**) are before and after stimulus delivery, respectively. The data in (**d)** and (**i**) were tested for statistical significance by repeated measures ANOVA, followed by Bonferoni's post-hoc comparisons. Scale bars in (**f), (l)** are 9µm and 8.5µm respectively. All data shown are mean±SEM.

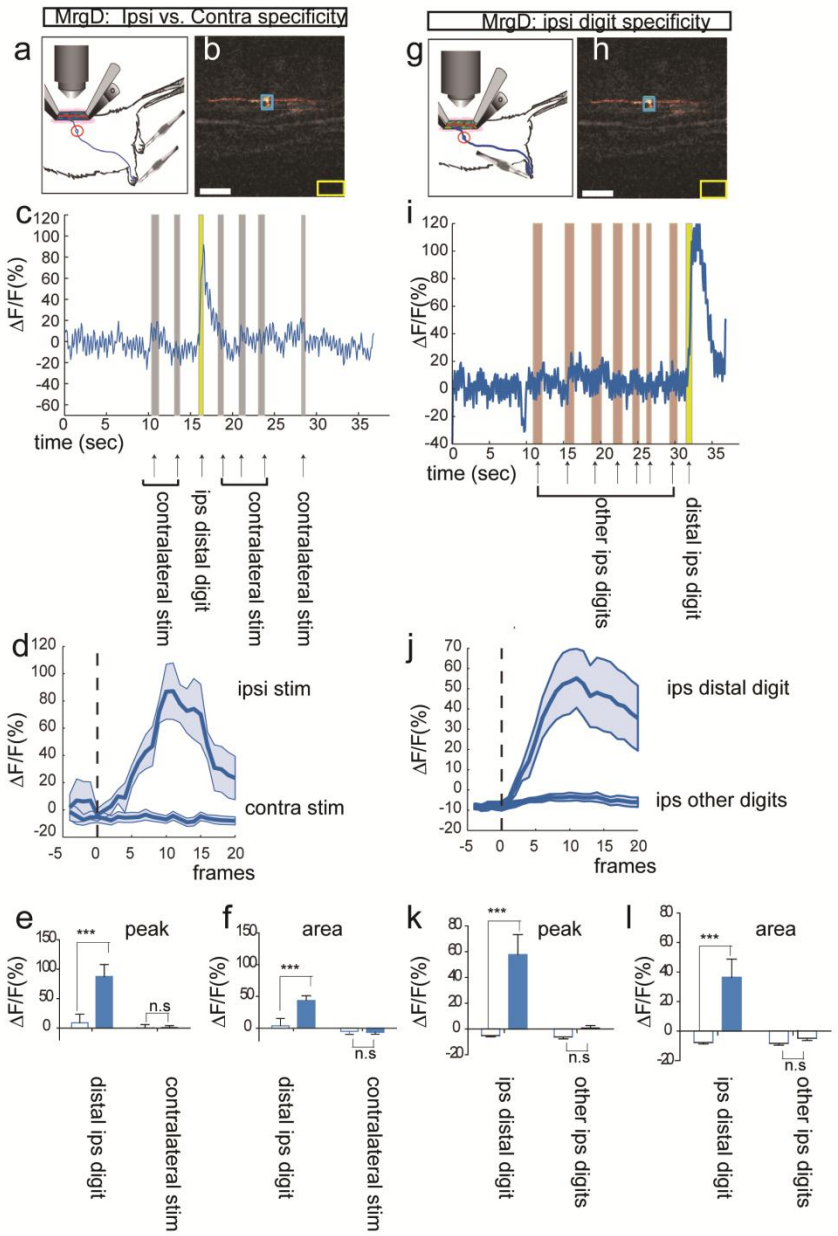

Supplementary Figure S6. Regional specificity of MrgprD$^+$ fiber activation by pinching stimuli. a, g, Schematics illustrating pinching stimuli. **b, h** ROIs used for imaging in (**c-i)**. Yellow rectangles (lower right in **b, h**) are regions used for background subtraction. **c**, Superimposed traces from the ROI in (**b**) in a single trial consisting of 7 pinch stimuli (yellow bar represents pinching in a specific ipsilateral digit where pinching evokes a response, gray bars represent pinching in contralateral digits). **d**, Trial average for response to pinching (n=3 trials, 1

stimulus/trial in a specific ipsilateral digit where pinching evokes a response and 8 stimuli in total in contralateral digits) from a single animal. **e, f** MPI $\Delta F/F_{peak}$ (**e**) or integrated area (**f**) calculated from the curves in (**d**). **i**, Superimposed traces from the ROI in (**h**) in a single trial consisting of 8 pinch stimuli (yellow bar represents pinching in a specific ipsilateral digit where pinching evokes a response, brown bars represent pinching in other ipsilateral digits). **j**, Trial average for response to pinching (n=3 trials, 4 stimuli in total in a specific ipsilateral digit where pinching evokes a response and 12 stimuli in total in other ipsilateral digits), from a single animal. **k, l,** MPI $\Delta F/F_{peak}$ (**k**) or integrated area (**l**) calculated from the curves in (**j**). Open and filled bars in (**e), (f), (k)** and **(l)** are before and after stimulus delivery, respectively. The data in (**e), (f), (k)** and **(l)** were tested for statistical significance by repeated measures ANOVA, followed by Bonferonni's post-hoc comparisons. All data shown are mean±SEM. Scale bars in (**b), (h)** are 15.6 μm.

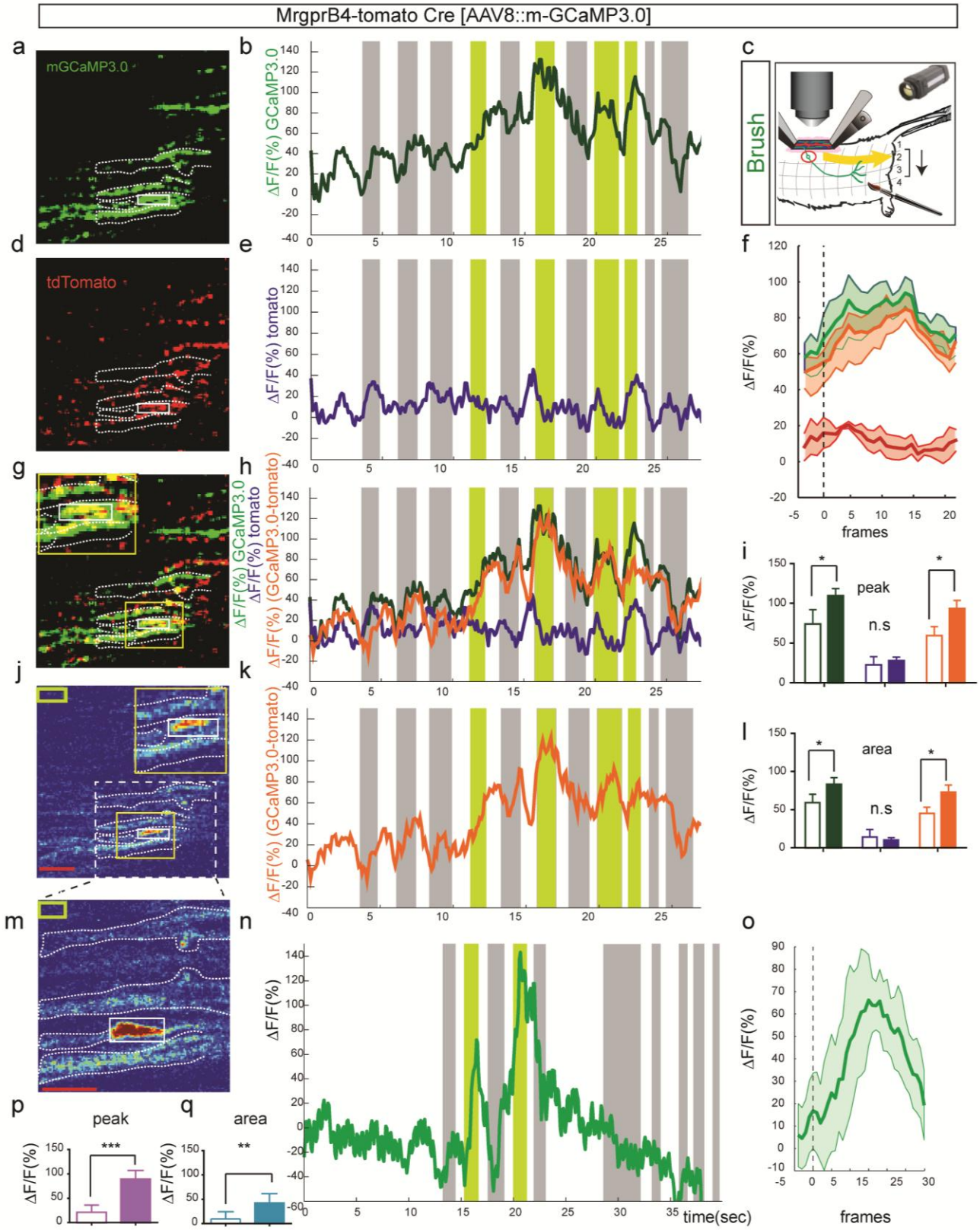

Supplementary Figure S7. Imaging activity during stroking in tdTomato^{+}MrgprB4 fibers.

(c) Schematic illustrating delivery of brushing stimulus in different zones. (**a, d, g, j**) Visualization, in the same field of view of (**a**) GCaMP3.0^{+} (before stimulation), (**d**) tdTomato^{+}, (**g**) superimposed expression of both fluorescent labels and (**j**) F pseudo-color representation of GCaMP3.0 signal from (**a**) during stimulation, in MrgprB4^{+} central afferent fibers. Insets in (**g**) and (**j**) are higher magnification views of yellow-boxed region. Scale bar (**j**, red) is 19.6 μm. White solid line rectangular boxes in **(a, d, g, j**) define region-of-interest (ROI) used for imaging studies in (**b, e, h, k**), in which GCaMP3.0^{+} and tdTomato^{+} fibers are indistinguishable at this level of resolution (**g**). ΔF/F responses in the indicated ROI from (**b**) G-CaMP3.0, (**e**) tdTomato, (**k),** GCaMP3.0 minus tdTomato and (**h**) superposition of (**b, e, k**), to brushing stimuli delivered to hairy skin (**c**). Yellow bars represent brushing in ipsilateral zone 1 (**c**), where stimulation evoked responses, and gray bars brushing in zones 2, 3, 4 and in the contralateral side where stimulation failed to produce calcium transients in the specific field of view. (**f**), Average ΔF/F responses to 4 brushing stimuli in zone 1, from a single animal in a single trial. (**i, l),** MPI $\Delta F/F_{peak}$ (upper) or integrated area (lower) calculated from the curves in (**f**), respectively. Open and filled bars are 5 frames before and 20 frames after stimulus delivery (vertical dashed line in (f)), respectively. (**m),** F pseudo-colored higher magnification field-of-view of the white dashed rectangular area in (**j**) during stimulation; scale bar 11.41 μm. (**n**), GCaMP3.0 ΔF/F responses to a single trial of brushing stimuli from the ROI in (**m**), which encloses the same fibers as the ROI in (**j**), but imaged at higher magnification. (**o**), Average responses to 5 brushing stimuli in zone 1 from a single animal in 4 trials, using the ROI in (**m**). (**p, q**), MPI $\Delta F/F_{peak}$ (left) or integrated area (right) calculated from the curve in (**o**). Open and filled bars are 5 frames before and 30 frames after stimulus delivery, respectively. All data shown are mean±SEM.

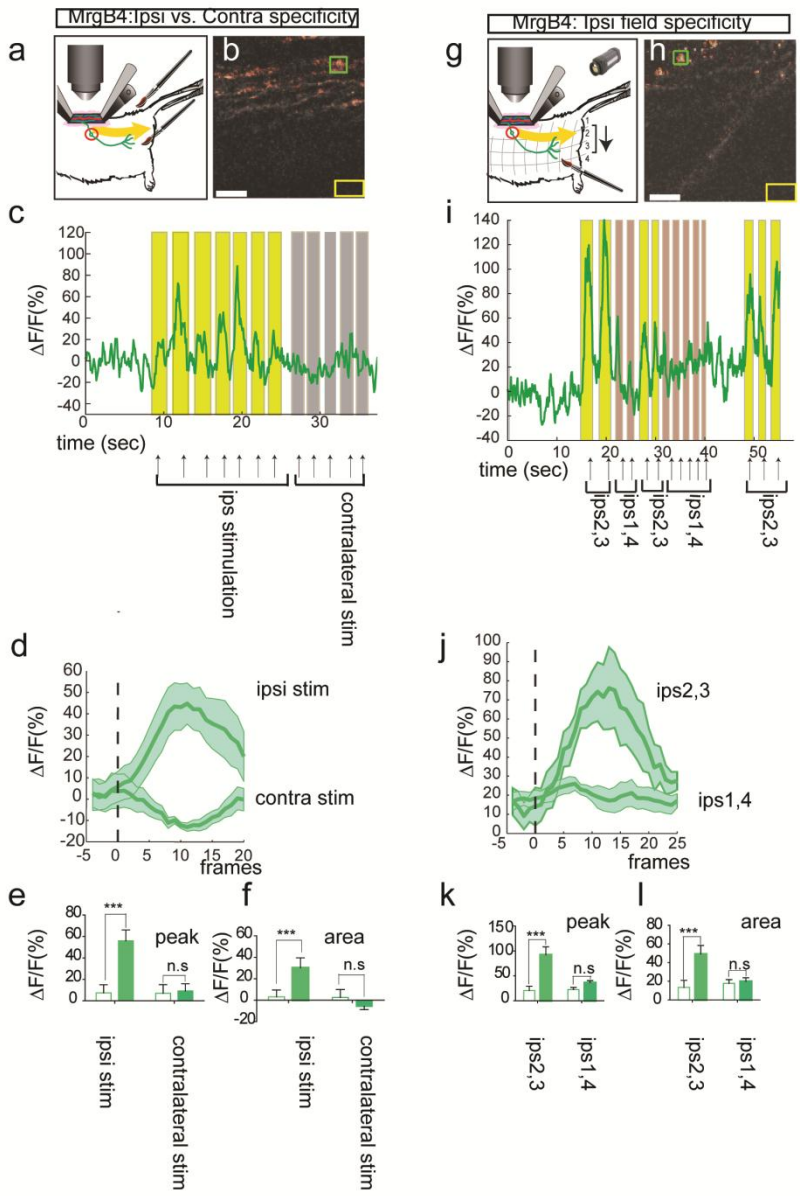

Supplementary Figure S8. Regional specificity of MrgprB4^{+} fiber activation by brushing stimuli. a, g, Schematics illustrating brushing stimuli. In (**g**), a red grid is projected onto the mouse delineating separate horizontal and vertical zones (see Supplementary Methods). **b, h** ROIs (green boxes) used for imaging in (**c-i)**. Yellow rectangles (lower right in **b, h**,) are region used for background subtraction. **c**, Superimposed traces from the ROI in (**b**) in a single trial consisting of 12 brushing stimuli (yellow bars represent brushing ipsilaterally that evokes a

response, gray bars represent contralateral brushing). **d**, Trial average for response to brushing (n=4 trials, 28 ipsilateral brushing stimuli and 22 contralateral brushes), from a single animal. **e, f,** MPI $\Delta F/F_{peak}$ (**e**) or integrated area (**f**) calculated from the curves in (**d**). **i**, Superimposed traces from the ROI in (**h**) in a single trial consisting of 14 brushing stimuli (yellow bars represent response inducing ipsilateral brushing in horizontal zones 2,3 and brown bars represent unresponsive ipsilateral brushing in horizontal zones 1,4). **j**, Trial average for response to brushing (n=1 trial, 7 brushing stimuli in responsive zones 2,3 and 7 brushing stimuli in the unresponsive zones 1,4), from a single animal. **k, l,** MPI $\Delta F/F_{peak}$ (**k**) or integrated area (**l**) calculated from the curves in (**j**). Open and filled bars in (**e), (f), (k)** and **(l),** are before and after stimulus delivery, respectively. The data in (**e), (f), (k)** and **(l),** were tested for statistical significance by repeated measures ANOVA, followed by Bonferoni's post-hoc comparisons. All data shown are mean±SEM. Scale bars in (**b), (h)** are 15 and 19 µm respectively.

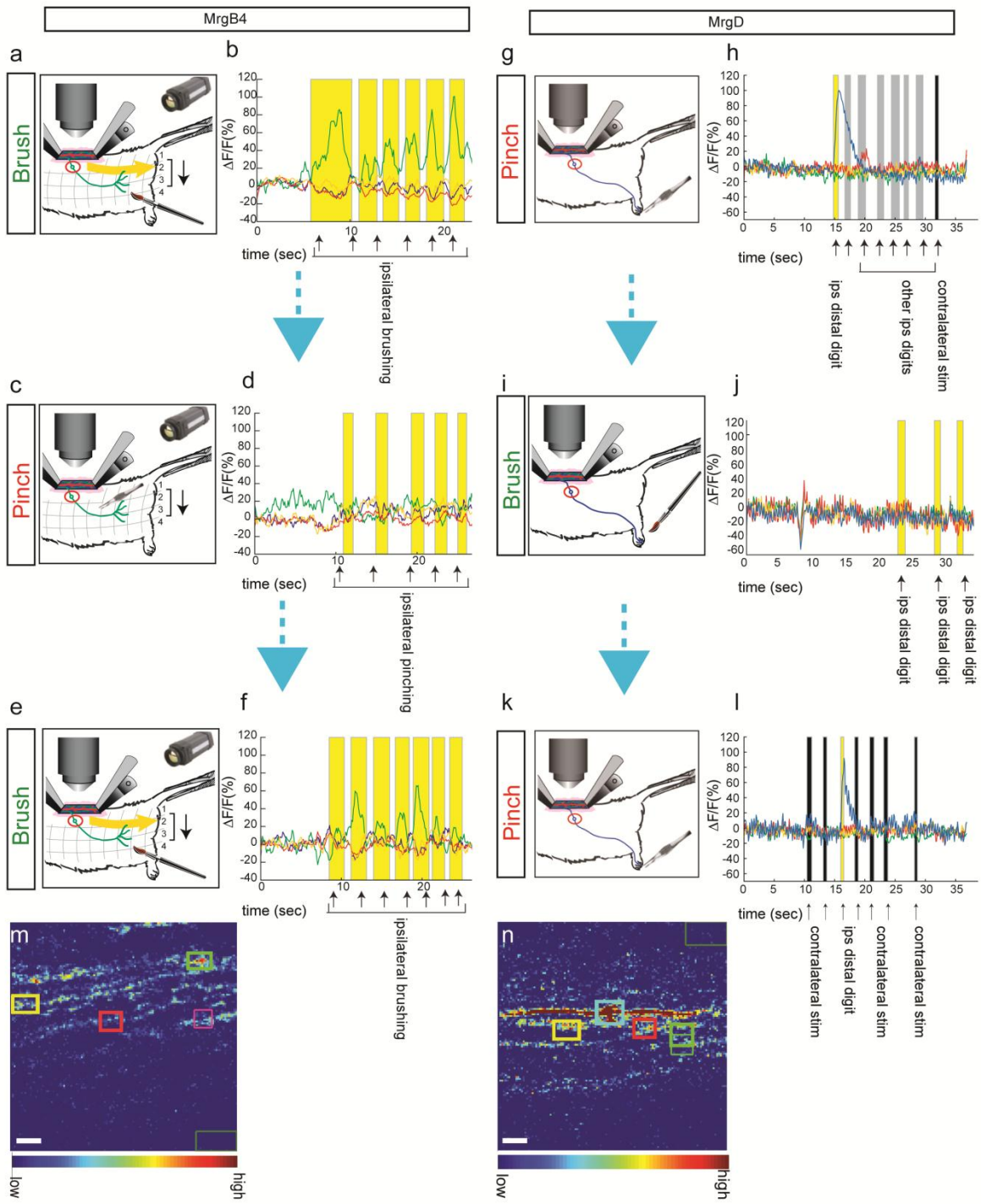

Supplementary Figure S9. Imaging activity in MrgprB4$^+$ and MrgprD$^+$ fibers during alternating, sequential delivery of stroking and pinching stimuli. **a, e, i**, Schematics illustrating brushing stimuli and **c, g, k**, schematics illustrating pinching stimuli. In (**a, c, e**) **a** red

grid was projected onto the mouse to delineate a series of horizontal and vertical zones (see Materials and Methods). **m**, ROIs used for imaging in (**b, d, f**); **n,** ROIs used for imaging in (**h, j, i**). Olive green rectangles in lower right (**m**) and upper right (**n**) are regions used for background substraction. **b, d, f**, Sequential trials from the same *MrgprB4-tdTomato-2A-Cre/GCaMP3.0* animal. **b**, Superimposed traces from different ROIs in the same field of view (**m**), in a single trial consisting of 6 brushing stimuli (yellow bars). **d,** Superimposed traces from the same ROIs (**m**) in a consecutive trial, consisting of 5 localized pinching stimuli, in the same zones (identified by the grid) where brushing stimulation evoked responses in (**b)** (yellow bars represent pinching stimuli). **f**, Superimposed traces from the same ROIs (**m**) in a consecutive trial consisting of 7 brushing stimuli (yellow bars). **h, j, l**, Sequential trials from the same *MrgprD-EGFPCre/GCaMP3* animal. **h**, Superimposed traces from different ROIs in the same field of view (**n**), in a single trial consisting of 8 pinching stimuli (yellow bar represents pinching in a specific ipsilateral digit where pinching evoked a response, gray bars represent pinching in other ipsilateral digits and black bar represent pinching in a contralateral digit). **j,** Superimposed traces from the same ROIs (**n**) in a consecutive trial consisting of 3 brushing stimuli (yellow bars) in the same digit where pinch stimulation evoked a response in (**h)**. **k**, Superimposed traces from the same ROIs (**n**) in a consecutive trial consisting of 7 pinch stimuli (yellow bars represents pinching in a specific ipsilateral digit where pinching evokes a response, black bars represent pinching in other contralateral digits). Scale bars in (m), (n) are 8.5 and 9 μm respectively.

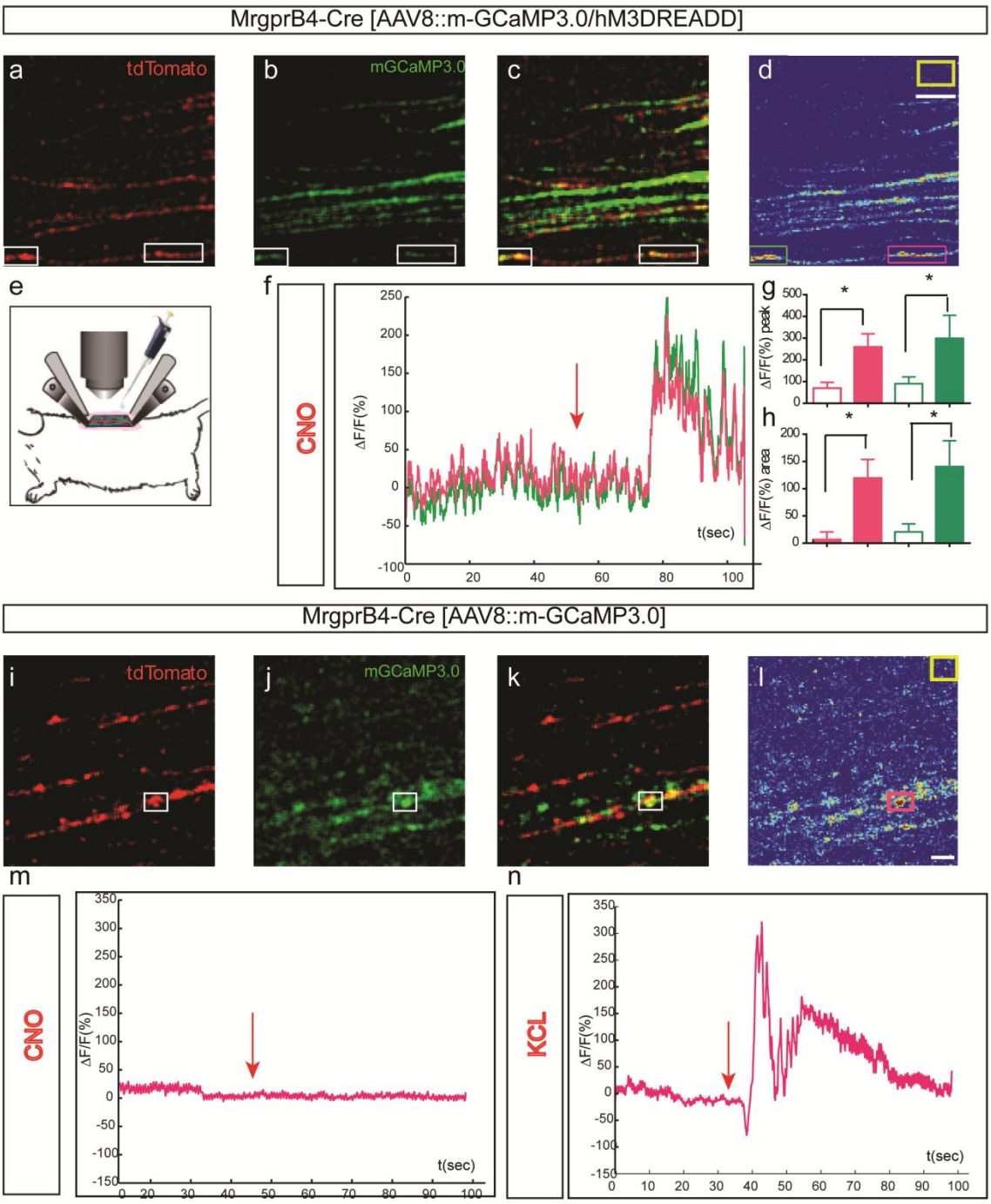

Supplementary Figure S10. MrgprB4^{+} fibers expressing hM3DREADD exhibit calcium transients in response to CNO.

(**e**), Schematic illustrating delivery of chemicals to the dorsal spinal cord of *MrgprB4-Cre* mice co-injected neonatally with Cre-dependent AAV8 viruses encoding CGaMP3.0 and/or

hM3DREADD. (**a-d** and **i-l**) illustrate MrgprB4^{+} central afferents in the same fields of view before (**a, b, c, I, j, k**) and after (**d, l**) chemical application, from AAV8:GCaMP3.0-injected MrgprB4-Cre mice with (**a-d**) or without (**i-l**) co-injection of hM3DREADD virus, respectively. (**a, i**), tdTomato; (**b, j**), GCaMP3.0; (**c, k**), merged expression of GCaMP3.0 and tdTomato; (**d, l**) F pseudocolor representation of GCaMP3.0 signal after the addition of CNO and KCL respectively. CNO application produced robust calcium transients in mice co-injected with both GCaMP3.0 and hM3READD viruses (**f**), whereas no CNO responses were seen in mice injected only with GCaMP3.0 viruses (**m**). As a positive control, the MrgprB4^{+} fibers in the same field of view (**l**), used to produce the plot in (**m**) showed robust activation after KCl application (**n**). Red arrows (**f, m, n,**) indicate time of stimulus delivery. White rectangles in (**a-c**), corresponding to green and pink rectangles in (**d**), indicate Regions-Of-Interest (ROIs) used to produce the pink and green traces in (**f**). White rectangles in (**i-k)**, corresponding to pink rectangle in (**l**), indicate ROI used to produce traces in **(m, n**). Yellow boxes in (**d, l**) indicate regions used for background subtraction. (**g, h**) Quantification of peak $\Delta F/F$ values (**g**) or integrated area (**h**), for the two ROIs (green and pink rectangles in (**d**) before (open bars) vs. after (filled bars) 4 consecutive CNO applications in the spinal cord of the same mouse (each CNO application is followed by washing with imaging solution). Application of imaging solution did not yield any responses. All data shown are mean±SEM.

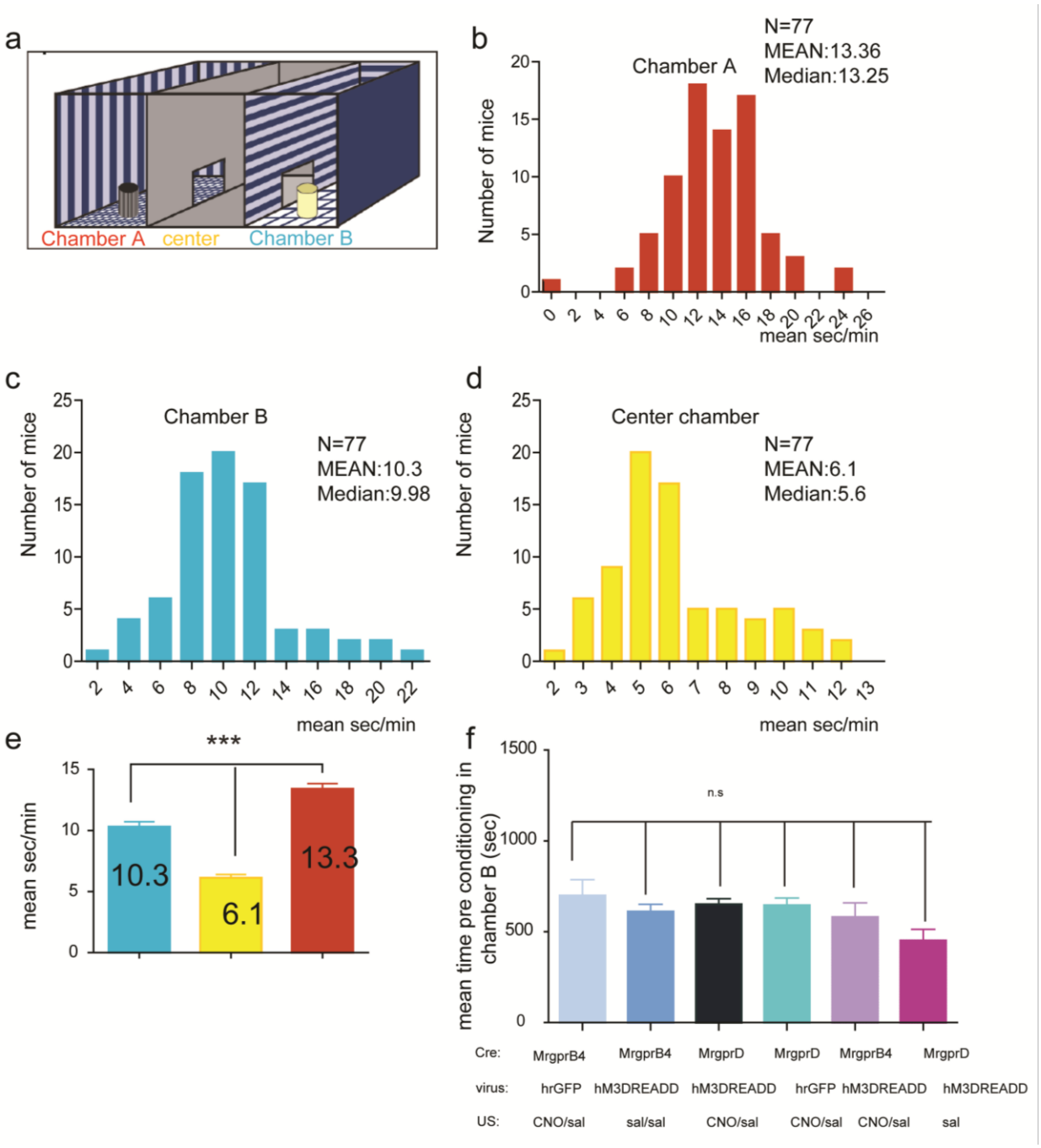

Supplementary Figure S11. Characterization of the apparatus used for the conditioned place preference.

(**a**) Schematic illustrating conditioning apparatus; Chamber A and Chamber B correspond to the histograms shown in (**b**) and (**c**), respectively. (**b, c, d**) Frequency histograms showing the

distribution of times (mean s/min) spent on each of the side chambers of the apparatus (**b, c**) and in the center chamber (**d**) during the 30 min pre-test session for all the mice used in the CPP and CPA assays. (**e**) Mean time (s/min) spent in each chamber of the apparatus by all mice used during the 30 min pre-test. $P<0.0001$ by repeated measures one way ANOVA followed by Bonferroni post tests. (**f**) One way ANOVA (followed by Bonferroni post tests) indicated no significant differences (all P values >0.05) between different groups in mean time spent in Chamber B (**c**) during the pre-test prior to conditioning (no apparatus bias across groups). There was also no significant difference (all P values >0.05) between groups for those mice for whom Chamber B was the I.N.P. chamber (80% of mice; not shown).

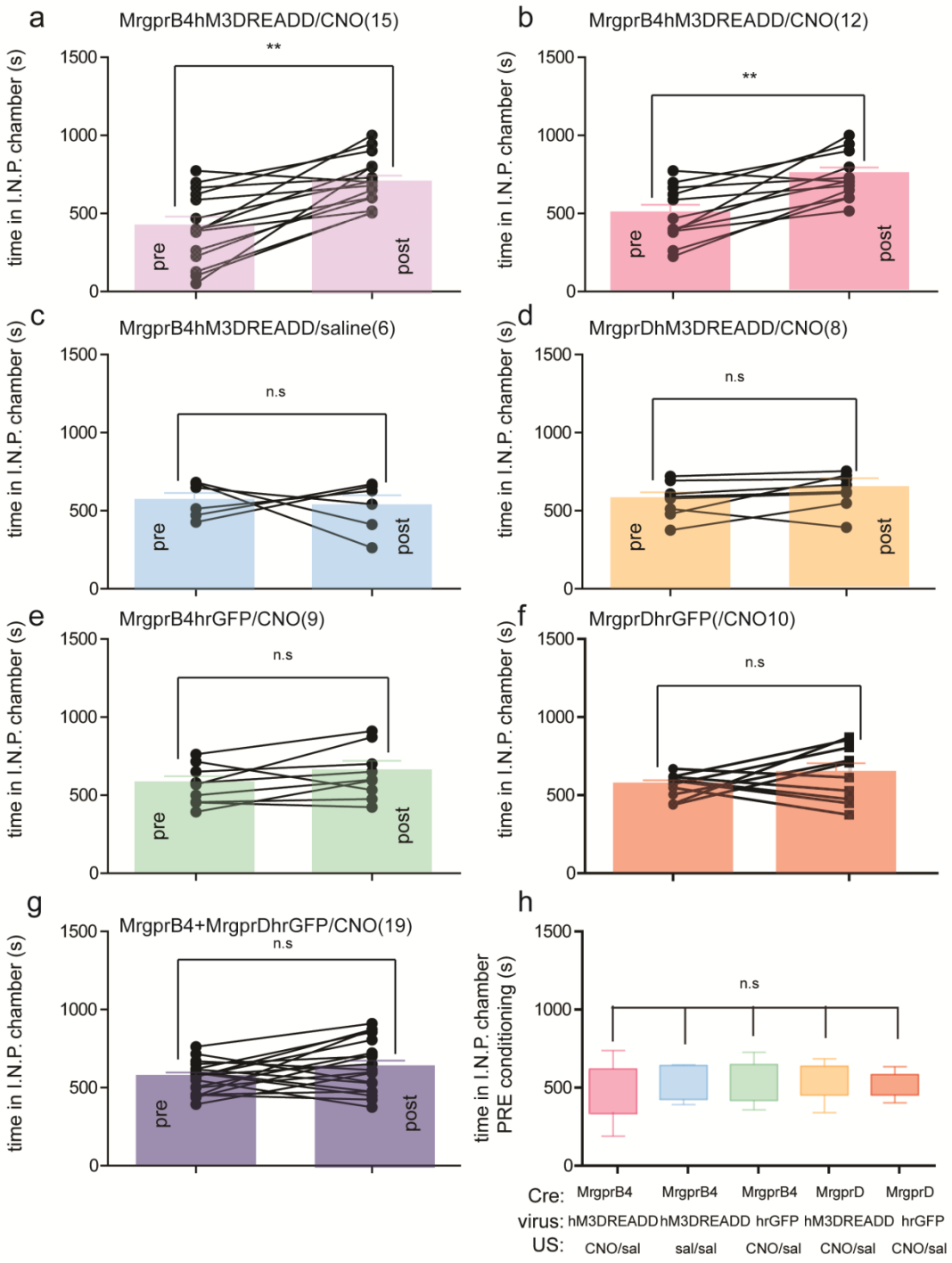

Supplementary Figure S12. Scatter-plot representation of the absolute time (s) spent pre- and post-conditioning for each mouse in the I.N.P. chamber in all groups.

Absolute time (sec) spent by each mouse in the I.N.P chamber pre- and post-conditioning with CNO (**a, b, d, e, f, g**) or saline (**c**). Data points corresponding to the same mouse pre- and post-conditioning are connected by solid black lines. The shaded bars indicate group averages; significant differences ($P<0.01$, as determined by independently performed paired t tests) between pre- and post-conditioning were found only in the experimental group (**a**) and (**b**) (MrgprB4-Cre/hM3DREADD mice conditioned with CNO in the I.N.P. chamber). In (**b**), all the mice in (**a**, n=15) were included except for those animals whose pre-test times in the I.N.P chamber were > or < 2 standard deviations ($P<0.046$) from the mean pre-test time of all combined mice; this resulted in exclusion of 3 mice that showed the lowest pre-test time in the I.N.P. chamber (**b,** n=12). Application of this same procedure to all other control groups resulted in no exclusion of any datapoints. This procedure should, if anything, bias the data away from showing an effect (by raising the mean pre-test score of the experimental group; compare mean pre-test scores in **a** vs. **b**), yet a statistically significant difference was still observed only in the experimental group (**b**). (**c-g**) Control groups. (**c**) MrgprB4-Cre/hM3DREADD mice conditioned with saline in both chambers (n=6); (**d**) MrgprD-Cre/hM3DREADD mice conditioned with CNO (n=8); (**e, f**) MrgprB4-Cre (**e**, n=9) and MrgprD-Cre (**f**, n=10) mice injected with a control virus (Cre-dependent AAV8::hrGFP) and conditioned in the I.N.P. chamber with CNO. (**g**) Combined data for all hrGFP-injected control mice n=19 (**e** and **f**). (**h)** One way ANOVA followed by Bonferroni post tests indicated no significant differences (all P values >0.05) in time spent in I.N.P chamber pre-conditioning between the groups in (**b, c, d, e, f**). A similar result was obtained using the groups in (**a, c, d, e, f**) (not shown). All data shown are mean±SEM.

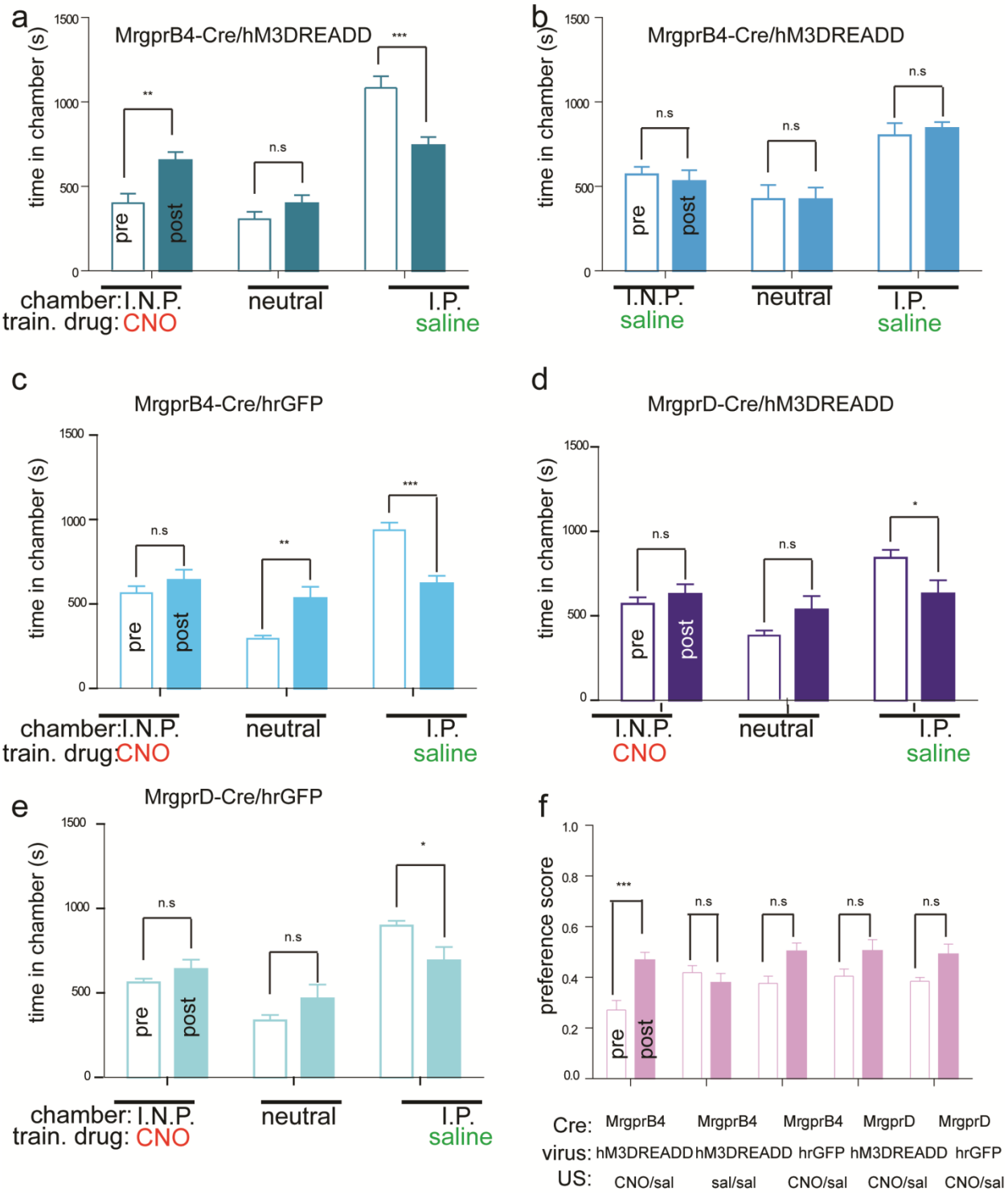

Supplementary Figure S13. Activation of MrgprB4-Cre/hM3DREADD neurons with CNO induces conditioned place preference. (**a-e**) Absolute time (sec) spent in each of the 3 indicated chambers for the experimental and control groups before ("pre") and after ("post") conditioning

with the indicated drug ("train. drug") (**a**) MrgprB4-Cre/hM3DREADD mice injected with CNO (n=15); (**b**) MrgprB4-Cre/hM3DREADD mice conditioned with saline in both chambers (n=6). (**c, e**) MrgprB4-Cre (**c**, n=9) or MrgprD-Cre (**e**, n=10) mice injected with a control virus (Cre-dependent AAV8::hrGFP) and conditioned in the I.N.P. chamber with CNO; (**d**) MrgprD-Cre/hM3DREADD mice injected with CNO and conditioned in the I.N.P (n=8). **f,** Preference score (=[time in I.N.P chamber]/[(time in I.N.P. chamber) +(time in I.P. chamber)]) for experimental and control groups. (**a-f**), (n.s., not significant), *,p<0.05, **, p<0.01, ***, p<.001. All data shown are mean±SEM. Statistical significance was tested by a repeated measures two way mixed ANOVA with group as the between subjects factor and pre/post scores as the within subjects factor. Detection of significant interactions {(**a**), p<0.0001, F(2,42)=22.29, (**b**), no significant interaction, (**c**), p<0.001, F(2,24)=17.08, (**d**), p<0.01, F(2,21)=6.074, (**e**), p<0.01, F(2,27)=5.630, (**f**), p<0.05, F(4,43)=2.851} and/or main effects {(**a**), group main effect, p<0.0001, F(2,42)=45.05, (**b**), group main effect, p<0.001, F(2,15)=52.48, (**c**), group main effect, p<0.001, F(2,24)=24.82, (**d**), group main effect, p<0.01, F(2,21)=9.209, (**e**) group main effect, p<0.001, F(2,27)=21.45} (**f**) pre/post main effect, p<0.0001, F(1,43)=19.70 was followed by a Bonferoni-corrected post hoc comparison of means. The non-significant trends to an increased preference score for *MrgprB4/hrGFP, MrgprD-Cre/hrGFP* and *MrgprD-Cre/hM3DREADD* mice in (**f**) reflects a decreased time in the saline-paired (I.P.) compartment, and corresponding increase in the time spent in the neutral compartment (see panels **c, d, e**), not a statistically significant increase in time spent in the CNO-paired (I.N.P.) compartment (the numerator in the preference score).

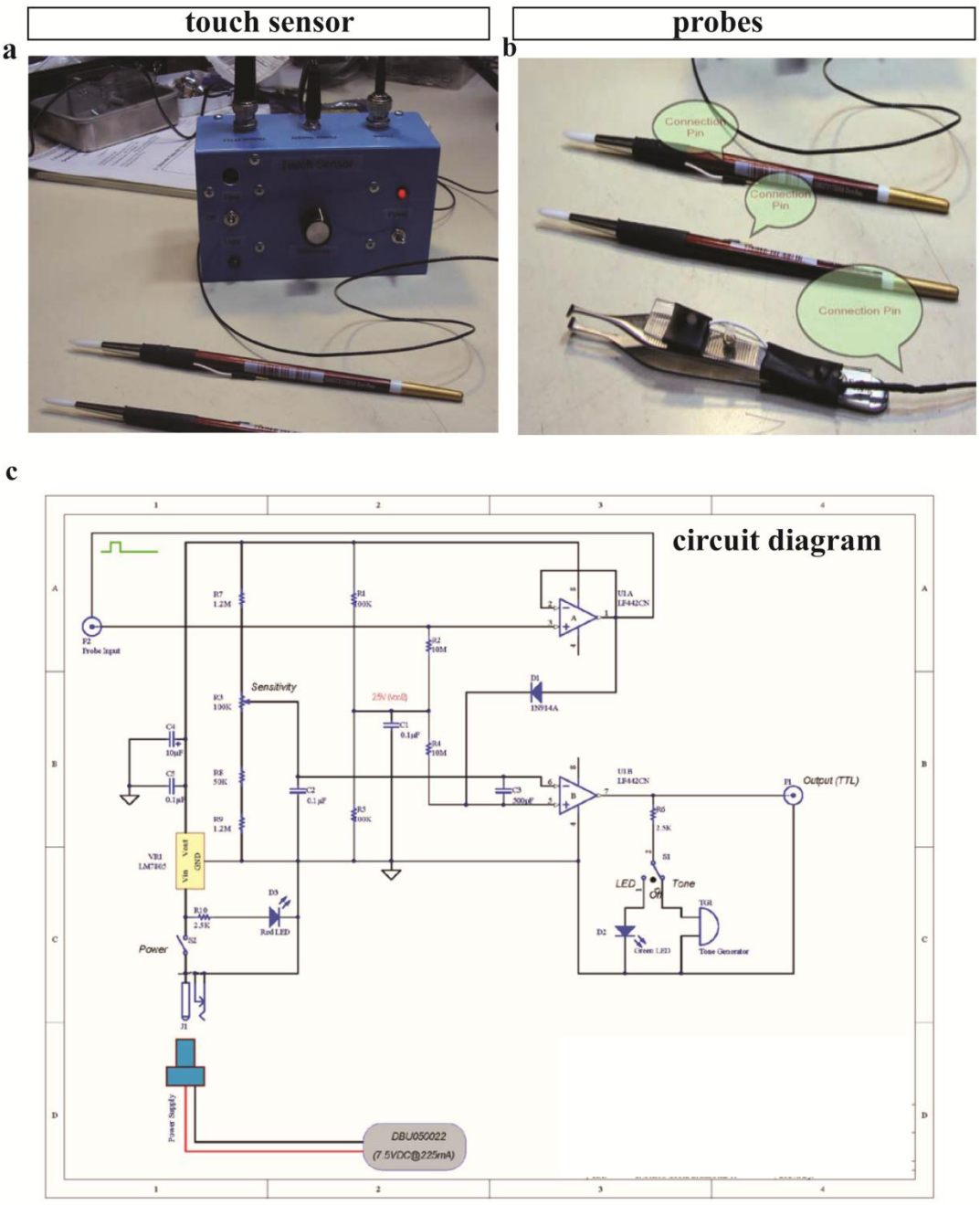

Supplementary Figure S14. Apparatus used for mechanical stimulation. Photos of the touch sensor amplifier box (**a**) and of the probes (paint brush and forceps) (**b**) used for mechanical stimulation during imaging. A circuit diagram of the touch sensor is shown in (**c**).

2.SUPPLEMENTARY TABLES

AAV plasmids tested for Imaging	Expression cell bodies	Expression central fibers
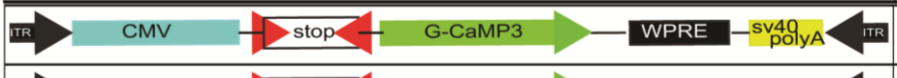	++	+
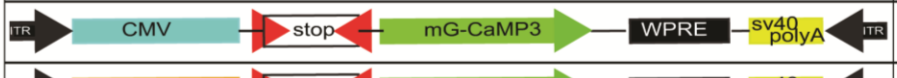	+	++
	low	low
	low	low
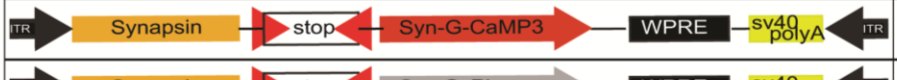	-	-
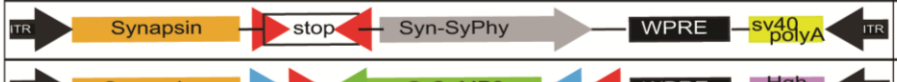	-	-
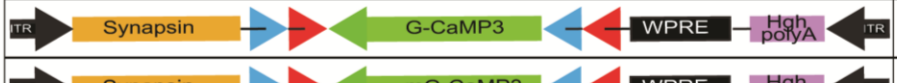	low	-
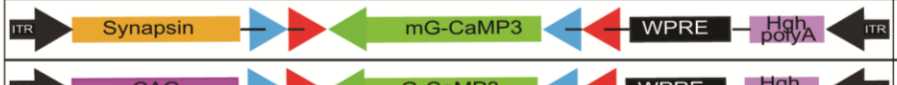	-	low
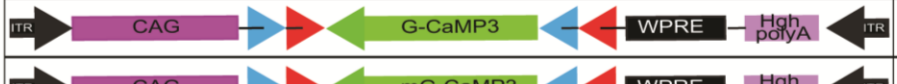	low	-
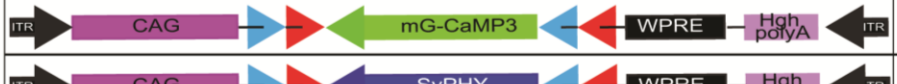	-	low
	-	-
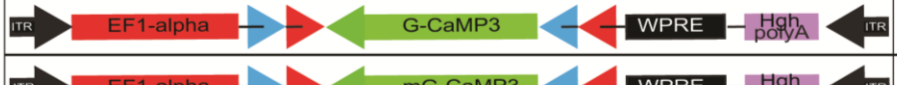	low	-
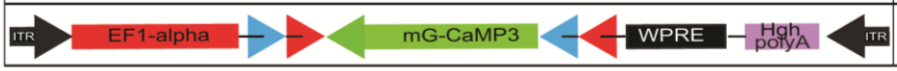	-	low

Supplementary Table 1. AAV constructs tested for Imaging. The use of CMV promoter and of the loxP-STOP-loxP cassette (rather than the FLEX design for Cre dependence; bottom 7 constructs) resulted in higher levels of expression in cell bodies and in the central fibers.

Genotype	Mouse#			
MrgDcre	1	2	3	4
Means +/-sem ΔF/F(peak) ROI1Before stim After stim	 29.77± 10.38 103.74± 5.12 P<0.001	 9.70±1.73 21.47± 2.75 P<0.001	 65.09± 9.10 108.60± 9.39 P<0.05	 20.72± 6.41 41.67± 8.26
Means +/-sem ΔF/F(peak) ROI2Before stim After stim	 25.24± 7.32 89.05± 4.77 P<0.001	 6.73±1.88 14.02± 2.26 P<0.05	 67.16± 8.95 108.41± 8.39 P<0.05	 30.17±11.48 60.05±18.15 P<0.05
#trials	4	6	7	8
ΔF/F(peak) Before and after stimulation ROI1, ROI2	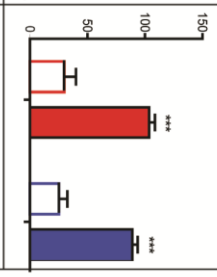	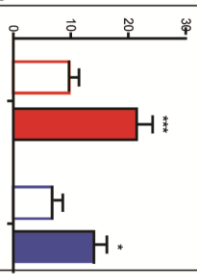	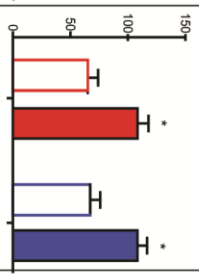	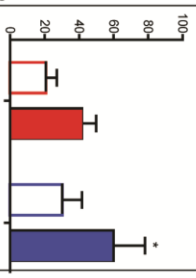

Supplementary Table 2. $\Delta F/F_{peak}$ responses in 4 MrgprD mice before and during pinching stimulation. The animals shown are in addition to the animal analyzed in Fig. 2h. Mice 1-3 are the same as those shown in Fig. 2j. Calcium transients were measured for two different ROIs in a given field of view. The data were tested for statistical significance by repeated measures ANOVA, followed by Bonferoni-corrected post hoc comparison of means.

Genotype	Mouse#				
MrgB4cre	1	2	3	4	5
Means +/-sem ΔF/F(peak) Roi1Before stim After stim	 4+/-2.17 48.01+/-9.21 P<0.05	 8.75+/1.96 32.27+/-3.3 P<0.001	 -4.79+/-2.61 37.23+/-10.31 P<0.001	 -14.8+/-3.94 43.94+/-7.79 P<0.001	 -6.02+/-2.29 23.44+/-4.61 P<0.01
Means +/-sem ΔF/F (peak) Roi2 Before stim After stim	 1.31+/-6.77 33.26+/-6.56 P<0.05	 24.4+/-2.52 42.5+/-2.47 P<0.001	 7.95+/-2.83 16.77+/-4.47 P<0.05	 -19.6+/-3.09 26.16+/-7.23 P<0.001	 5.89+/-2.79 17.47+/-6.69 P<0.01
#trials	2,5	13	14	14	5
ΔF/F(peak) Before and after stimulation Roi1, Roi2	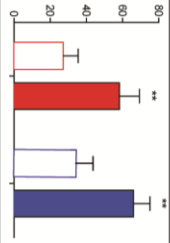	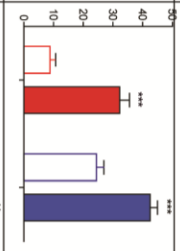	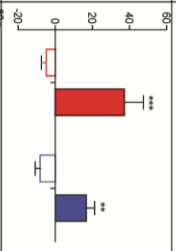	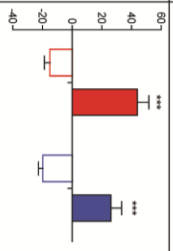	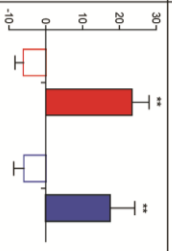
MrgB4cre	6	7	8	9	10
Means +/-sem ΔF/F (peak) Roi1Before stim After stim	 -2.62+/-1.15 15.62+/-3.24 P<0.001	 2.41+/-2.32 57.96+/-8.97 P<0.001	 8.68+/-2.44 25.67+/-3.46 P<0.05	 27.34+/7.45 74.6+/-13.96 P<0.05	 -14.97+/-1.83 5.97+/-4.42 P<0.001
Means +/-sem ΔF/F (peak) Roi2 Before stim After stim	 2.65+/-1 4 26.91+/- 3.06. P<0.001	 -8.35+/-2.17 19.95+/-5.62 P<0.01	 13.32+/-1.89 26.68+/-2.38 P<0.001	 40.7+/-5.73 89.62+/-12.64 P<0.05	 -6.22+/-3.33 15.82+/-4.52 P<0.001
#trials	10	16	14	6	8
ΔF/F(peak) Before and after stimulation Roi1, Roi2	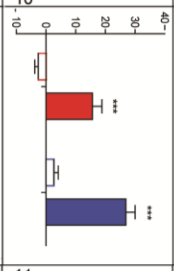	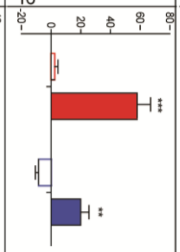	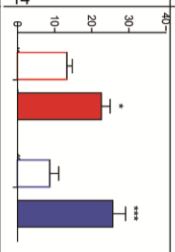	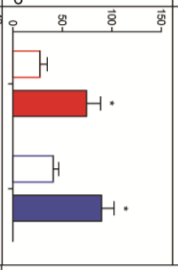	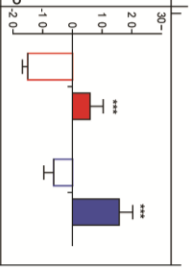
MrgB4cre	11a	11b	12		
Means +/-sem ΔF/F(peak) Roi1Before stim After stim	25.37+/-16.72 78.28+/-16.06 P<0.05	23.17+/-13.38 102.77+/-16.05 P<0.01	27.08+/-8.42 58.32+/-10.94 P<0.01		
Means +/-sem ΔF/F(peak) Roi2 Before stim After stim	37.26+/-15.74 99.81+/-19.32 P<0.05	67.68+/-18.37 167.23+/-34.7 P<0.01	34.24+/-9.46 65.97+/-9.22 P<0.01		
#trials	3	3	10		
ΔF/F(peak) Before and after stimulation Roi1, Roi2	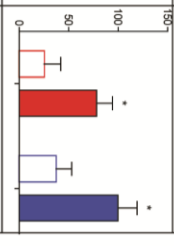	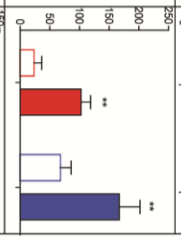	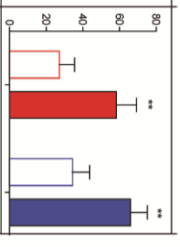		

Supplementary Table 3. $\Delta F/F_{peak}$ responses in 12 MrgprB4 mice before and during stroking stimulation. The animals shown are in addition to the animal analyzed in Fig. 3h and Supplementary Fig. 7. Mice 7, 1 and 12 correspond to mice 1, 2 and 3 respectively as shown in Fig. 3j. Calcium transients were measured for two different ROIs in a given field of view. The data were tested for statistical significance by repeated measures ANOVA, followed by Bonferoni-corrected post hoc comparison of means.$\Delta F/F_{peak}$ responses in 11a and 11b referred to measurements in two different fields of view in the same animal.

3.SUPPLEMENTARY DISCUSSION

Supplementary Discussion 1. The inability to detect activation of MrgprB4 neurons by mechanical stimuli *ex vivo* could be due to shaving the skin in such preparations[26], which may reduce the mechanical force that can be applied via bending of hairs during stroking, or more likely to the absence of underlying connective tissue, dermis and musculature in the skin explant, which makes it impossible to apply the same force or deformation as can be applied *in vivo*.

4. SUPPLEMENTARY NOTES

Supplementary Note 1. MrgprB4$^+$ neurons are distinct from a recently characterized population of tyrosine hydroxylase (TH)-positive C-fiber low-threshold mechanoreceptors (C-LTMRs), which do not express *Mrgprs* or bind IB4[9]. In isolated skin-nerve preparations, *MrgprB4*-expressing neurons (identified using an *EGFP* reporter; see Methods) responded neither to punctate stimulation using von Frey filaments (1-200 mN force), nor to gentle stroking with a paintbrush (0/25 neurons tested; see Methods), nor did they respond to thermal or to a cocktail of chemical stimuli. By contrast, *MrgprD*-expressing neurons were activated by von Frey filaments

by forces up to 100 mN in such preparations[10], consistent with a requirement of these neurons for normal behavioral responses to noxious mechanical stimulation in vivo[12].

Supplementary Note 2. A potential drawback of introducing exogenous genes into primary cutaneous sensory neurons in vivo by viral transduction is that infection of these neurons typically requires injection into the periphery, sciatic nerve or dorsal root ganglia (DRG)[40]. This yields a highly localized distribution of infected cells whose peripheral receptive fields may be equally restricted, conflating the problems of stimulus identification and receptive field localization. To circumvent this, we confirmed and extended a report suggesting that intra-peritoneal (i.p.) injection of adeno-associated virus of serotype 8 (AAV8) into neonatal pups results in widespread infection of DRG neurons in adults[28]. I.p. injection of P0-P2 *MrgprB4-tdTomato-2A-Cre* mouse pups with a Cre-dependent AAV8 expressing either cytoplasmic or membrane-tethered forms of GCaMP3.0 (mGCaMP3.0; see Supplementary Table 1 and Methods) under the control of the cytomegalovirus (CMV) promoter indeed yielded effective expression of the virally encoded GECI. Expression in MrgprB4$^+$ neurons was both relatively efficient ([viral GCaMP3.0$^+$, tdTomato$^+$/tdTomato$^+$] = 0.62±0.06; mean±SEM, n=24 sections), and specific in that the majority of GCaMP3.0$^+$ cells were tdTomato$^+$ ([viral GCaMP3.0$^+$, tdTomato$^+$/ GCaMP3.0$^+$] = 0.62±0.05). The incomplete overlap likely reflects variable levels of *MrgprB4-tdTomato-2A-Cre* expression and the fact that low levels of Cre (and therefore perhaps undetectable levels of tdTomato) can lead to recombination1[41]. A similar level of specificity was observed in MrgprD-EGFPCre mice infected with a Cre-dependent hrGFP AAV (see Fig. 1a, b, d and Suppl. Fig. 2a-c,g; [viral hrGFP$^+$, EGFPCre$^+$/hrGFP$^+$] = 0.62±0.036, n=9).

Supplementary Note 3. Anaesthetized mice were mounted under a two-photon microscope (Prarie Instruments, Inc.) in a suspension system designed to minimize breathing-associated

movement artifacts[29], and imaged ~100-250 μm below the pia through an agarose-covered dorsal laminectomy covering 2 lumbar segments[30] (L1-L3 or L2-L4) (Fig. 1f; see Materials and Methods). Similar results were obtained using either a membrane-tethered form of GCaMP3.0 (mGCaMP3.0) or a cytoplasmic form of the GECI (see Supplementary Table 1).

Supplementary Note 4. Calcium responses in MrgprD$^+$ neurons were activated by spinal application of α,β Me-ATP (Supplementary Fig. 3, MPI $[\Delta F/F]_{peak}$ = 249±54%, MLP = 16.3±1.3, mean±range, n=2), consistent with previous studies indicating that these neurons are ATP-responsive[15]. Calcium transients were evoked in MrgprD$^+$ fibers by injection of α,β Me-ATP into the glabrous skin of the hind paw (Fig. 1k, m; MPI $[\Delta F/F]_{peak}$=137±51%, MLP = 25.7±10.5 sec, n=3) and in MrgprB4$^+$ fibers by injection of α,β Me-ATP into the dorsal (hairy) skin of the hindpaw (Fig. 1l, n; MPI $[\Delta F/F]_{peak}$ = 142±0.6%, MLP = 21.9±12.6 sec, n=3). As an additional validation of our ability to image activation of MrgprB4-expressing fibers by a peripherally injected specific ligand, we mis-expressed TrpV1 in these fibers (which normally do not express this channel[7]) by crossing *MrgprB4-Cre* mice to *Rosa26-loxP-STOP-loxP-TrpV1* mice[42], and injected them neonatally with Cre-dependent AAV encoding GCaMP3.0. Peripheral injection of adult *MrgprB4-Cre*; *Rosa26-loxP-STOP-loxP-TrpV1* mice with capsaicin induced robust calcium transients, while no such signals were observed in control *MrgprB4-Cre* mice injected with capsaicin (Supplementary Fig. 4).

Supplementary Note 5. In MrgprD::GCaMP3.0 mice, pinching of the contralateral hind paw evoked no responses in MrgprD$^+$ fibers activated by stimulation of the ipsilateral paw (Supplementary Fig. 6a-f). Moreover, Ca^+ transients in a specific ROI were evoked only when pinching was applied to a particular digit of the ipsilateral hindpaw, and not to other digits (Supplementary Fig. 6g-l), suggesting that the responses were specific to a given peripheral

receptive field. The ΔF/F responses for a given ROI were reproducible across trains of stimuli within a trial (Fig. 2d), as well as across multiple trials in a given mouse (Fig. 2e, h), and were independently observed in 5 different mice (MPI $[\Delta F/F]_{peak}$ = 47.4±12.7%, n=5 mice; Fig. 2j and Supplementary Table 2).

Supplementary Note 6. As in the case of the MrgprD$^+$ fibers, Ca^+ transients elicited in MrgprB4$^+$ fibers by stroking the skin were specific for a particular ROI in a given field of view (Fig. 3c-d and Supplementary Fig. 5g-i), occurred synchronously with the delivery of stimulation (Fig. 3d, light blue bars), and were evoked by stimulating the ipsilateral but not the contralateral side (Supplementary Fig. 8a-f). Moreover, Ca^+ transients were evoked by stroking certain regions of the skin (identified by projecting a light grid onto the mouse; see Methods), but not by stroking other, neighboring regions (Supplementary Fig. 8g-l). Although the responses were somewhat variable in magnitude, they were reproducible across trains of stimuli in a given trial (Fig. 3d and Supplementary Fig. 7), multiple trials in a given mouse (Fig. 3e, h, green bars; MPI $[\Delta F/F]_{peak}$ = 38.8±4%, n=5 trials), and were observed in multiple animals (MPI $[\Delta F/F]_{peak}$ = 42.5±5.8%, mean±SEM, n=13 mice; Fig. 3j and Supplementary Table 3).

Supplementary Note 7. Spinal application of CNO was employed to image activation of hM3DREADD and GCaMP3.0-expressing MrgprB4$^+$ fibers. The low probability of double-infection of individual MrgprB4$^+$ neurons with both the GCaMP3.0 and hM3DREADD Cre-dependent viruses (~30%), taken together with the difficulty of identifying sites for focal peripheral injection corresponding to specific MrgprB4$^+$ central afferent fibers visualized in the spinal cord, precluded peripheral delivery of CNO for this assay.

Supplementary Note 8. MrgprB4::hM3DREADD mice also showed a statistically significant positive “difference score” (time spent in the specified chamber after conditioning- before

conditioning) for the CNO-paired (I.N.P.) chamber (Fig. 4e, j; 253±66 sec increase in the CNO-paired chamber vs. -340±74 sec decrease in the saline-paired chamber, $p<0.01$; see Methods). No significant change in the difference score for the I.N.P. chamber was observed when a cohort of mice expressing a neutral reporter (hrGFP) in either MrgprB4$^+$ or MrgprD$^+$ neurons was conditioned with CNO (Fig. 4f, n=9 and Fig. 4i, n=10), or when mice expressing hMDREADD were conditioned using saline in both chambers (Fig. 4g, n=6; see Supplementary Fig. 13b-e for absolute times spent in each chamber for each control group). A direct comparison of difference scores in the I.N.P. chamber showed that only the experimental group exhibited a statistically significant positive shift (Fig. 4j, $p<0.01$). The experimental, but not the control groups, also showed a statistically significant increase in their preference score for the I.N.P. chamber (time spent in the CNO/I.N.P. chamber divided by total time spent in the two test chambers; 195±86% increase, $p<0.001$ pre vs. post; Supplementary Fig. 13f).

Supplementary Note 9. In Figure 2, for calculating $\Delta F/F$ $[(F_{av}-F_0)/F_0]$, F_0 is the average of the first 10 frames of the recording period (see Methods). Since the baseline gradually declines during a trial (**d, f**), some $\Delta F/F$ values are <0 in unresponsive ROIs or in the immediate pre-stimulus period (left of dashed lines in **e, g**).

Supplementary Note 10. In Figure 4c, d, detection of a significant interaction: (**c**, $F(2,42)=22.29$, $p<0.0001$; **d**, no significant interaction); and/or main effect: (**c**, $F(2,42)=45.05$, $p<0.0001$; **d**, $F(1,43)=6.355$, $p=0.01$) by ANOVA was followed by a Bonferroni post-hoc test.

REFERENCES FOR SUPPLEMENTARY INFORMATION

40 Xu, Y., Gu, Y., Wu, P., Li, G.-W. & Huang, L.-Y. M. Efficiencies of transgene expression in nociceptive neurons through different routes of delivery of adeno-associated viral vectors. *Human gene therapy* **14**, 897-906, doi:10.1089/104303403765701187 (2003).

41 Yizhar, O. *et al.* Neocortical excitation/inhibition balance in information processing and social dysfunction. *Nature* **477**, 171-178, doi:nature10360 [pii]10.1038/nature10360 (2011).

42 Arenkiel, B. R., Klein, M. E., Davison, I. G., Katz, L. C. & Ehlers, M. D. Genetic control of neuronal activity in mice conditionally expressing TRPV1. *Nat Methods* **5**, 299-302, doi:10.1038/nmeth.1190 (2008).